Diabetes, Metabolic Syndrome and Obesity

Dovepress

open access to scientific and medical research

Open Access Full Text Article

ORIGINAL RESEARCH

MicroRNA-204-5p Ameliorates Renal Injury via Regulating Keap1/Nrf2 Pathway in Diabetic Kidney Disease

Jiajia Dong[1], Mengyu Liu[1], Yawei Bian[1,2], Wei Zhang[1], Chen Yuan[1], Dongyun Wang[1], Zihui Zhou[1], Yue Li[1], Yonghong Shi[1,2]

[1]Department of Pathology, Hebei Medical University, Shijiazhuang, People's Republic of China; [2]Hebei Key Laboratory of Kidney Disease, Shijiazhuang, People's Republic of China

Correspondence: Yonghong Shi, Department of Pathology, Hebei Medical University, No. 361 East Zhongshan Road, Shijiazhuang, Hebei, 050017, People's Republic of China, Tel +86 311 86266647, Email yonghongshi@163.com

Background: Diabetic kidney disease (DKD) is characterized by renal fibrosis, and the pathogenesis of renal fibrosis is still not definitely confirmed. MiR-204-5p plays an important role in the regulation of fibrosis, autophagy and oxidative stress. In this study, we aimed to investigate the role of miR-204-5p on renal damage in diabetic kidneys and the underlying mechanisms involved.

Methods: In vivo, AAV-Ksp-miR-204-5p mimics were injected into mice via tail vein. In vitro, high glucose-induced HK-2 cells were treated with miR-204-5p inhibitor, miR-204-5p mimics, ATG5 siRNA, tertiary butyl hydroquinone (TBHQ), ML385, or 3-Methyladenine (3-MA). FISH and qRT-PCR were used to detect miR-204-5p expression. The expressions of protein and mRNA were detected by Western blotting, immunofluorescence, immunohistochemistry and qRT-PCR. The concentration of fibronectin in HK-2 cells culture medium was detected by ELISA.

Results: The expression of miR-204-5p in diabetic kidneys was significantly inhibited than that in control group. Delivering miR-204-5p mimics increased miR-204-5p expression, improved renal function, inhibited renal fibrosis and oxidative stress, and restored autophagy in db/db mice. In vitro, the expression of miR-204-5p was inhibited by HG treatment in HK-2 cells. MiR-204-5p mimics effectively increased miR-204-5p expression and reduced fibronectin and collagen I expression, restored autophagy dysfunction, and increased Nrf2 expression, whereas these alterations were abrogated by Nrf2 inhibitor ML385, autophagy inhibitor 3-methyladenine (3-MA, 5 mM) treatment or ATG5 siRNA transfection in HG-induced HK-2 cells. In addition, miR-204-5p inhibitor significantly inhibited miR-204-5p expression and aggravated HG-induced fibronectin and collagen I expression, autophagy dysfunction, and decreased Nrf2 expression, while these alterations were abolished by Nrf2 activator TBHQ. Furthermore, the binding of miR-204-5p with Keap1 was confirmed by luciferase reporter assay and miR-204-5p negatively regulated Keap1 expression, resulting in the activation of Nrf2 pathway.

Conclusion: MicroRNA-204-5p protects against the progression of diabetic renal fibrosis by restoring autophagy via regulating Keap1/Nrf2 pathway.

Keywords: diabetic kidney disease, fibrosis, miR-204-5p, Keap1, Nrf2, autophagy

Introduction

Millions of people are diagnosed with prediabetes or diabetes every year.[1] With the increasing prevalence of diabetes mellitus, diabetic kidney disease (DKD) has become the leading cause of chronic kidney disease (CKD) and end-stage renal disease (ESRD).[2] The current therapies of controlling blood pressure and glucose levels only show a restrained efficiency in retarding the progression of DKD, resulting in many patients continuing to deteriorate toward ESRD.[3] Therefore, there is an urgent need to develop effective treatments to halt the progression of DKD.

Renal fibrosis is a critical pathological change associated with DKD. Some studies have reported that renal tubular change has been an essential predictor of kidney impairment in late-stage diabetic kidney disease, including the degree of

Received: 27 September 2023
Accepted: 21 December 2023
Published: 5 January 2024

Graphical Abstract

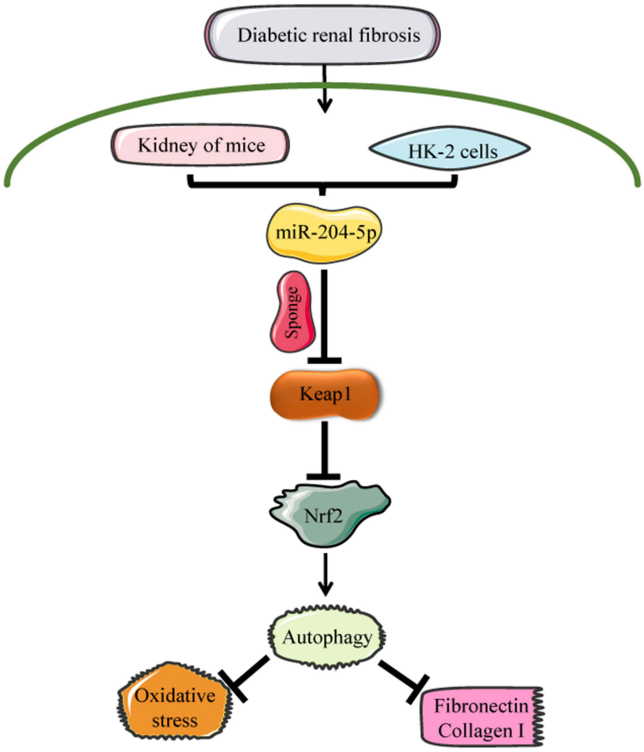

interstitial fibrosis and renal tubular atrophy (IFTA) score.[4] Several molecular pathways are associated with the pathogenesis of renal fibrosis,[5] including inflammation,[6] endoplasmic reticulum stress,[7] oxidative stress,[8] and autophagy.[9] Autophagy is an evolutionarily conserved homologous cellular process that plays a vital role in the degradation of damaged organelles and abnormal proteins to maintain cellular metabolism. Autophagy deficiency or absence has been observed in DKD, and restoration of autophagy is a new therapeutic strategy.[10]

Recent studies have shown a close connection between autophagy and oxidative stress.[11] Oxidative stress promotes the progression of DKD and leads to the abnormal accumulation of carbohydrates,[12] nucleic acids,[13] and proteins,[14] which are necessary for removal by autophagy for maintaining cellular homeostasis.[15] Sustained oxidative stress could impair autophagy, which aggravates oxidative damage. Nuclear factor erythroid 2-related factor 2 (Nrf2) is a key regulator of cellular homeostasis and regulates the expression of various cytoprotective genes.[16] A study has reported that inducing Nrf2 improved HG-induced oxidative stress and activated autophagy, which contributed to protecting kidneys against the damage of hyperglycemia.[17] Kelch-like ECH-associated protein 1 (Keap1) controls the degradation of Nrf2 to restrain its transcription activity in physiological conditions.[18] The study has shown that the inactivation of Keap1 protein may activate Nrf2 pathway, thus preventing the progression of DKD.[19]

MicroRNAs (miRNAs) are short non-coding RNAs that participating in fundamental biological processes by targeting functionally related gene networks.[20] The abnormal expressions of miRNAs are associated with many pathological conditions, including multifactorial and monogenic conditions.[21] MiRNAs are new targets for treatment and intervention in various human diseases and are emerging as molecular tools for non-mutation therapies.[22] A study has reported that miR-204-5p exhibited the most significant down-regulation among all detected miRNAs by small RNA deep-sequencing analysis of renal biopsy specimens from patients with hypertensive nephrosclerosis.[23] MiR-204-5p was one of the miRNAs with the most abundant expression in human kidneys, and abnormal miR-204-5p expression plays a pathogenic role in DKD.[24] A study has shown that miR-204-5p regulates Nrf2/ARE signaling pathway to participate in

the progression of cancer disease.[25] However, whether miR-204-5p is involved in the progression of DKD by regulating Keap1/Nrf2 has not been reported.

In the current study, we explored whether miR-204-5p is involved in renal fibrosis via Keap1/Nrf2 signaling pathway in DKD. In order to increase the expression of miR-204-5p, AAV-Ksp-miR-204-5p mimics were injected into mice via tail vein. We found that miR-204-5p protected against DKD through autophagy-restoring via regulating Keap1/Nrf2 signaling pathway.

Materials and Methods

Antibodies and Reagents

Collagen I, Nox4, and 8-hydroxydeoxyguanosine (8-OHdG) antibodies were obtained from ImmunoWay (Hong Kong, China). The antibodies against LC3 and HO-1 were obtained from Abcam (Cambridge, UK). Fibronectin, Nrf2, Keap1, β-actin, Histone H3, autophagy-related 5 (ATG5), GAPDH, and P62 antibodies were obtained from Proteintech (Chicago, IL). MiR-204-5p mimics and miR-204-5p inhibitor were obtained from RuiBio Corp. (Guangzhou, China). Tertiarybutylhydroquinone (TBHQ), 3-methyladenine (3-MA), and ML385 were purchased from Solarbio (Beijing, China). The ATG5 siRNA was synthesized by GenePharma (Suzhou, China). Fibronectin and 8-OHdG ELISA Kits were obtained from Elabscience Biotechnology (Wuhan, China).

Mice

Male 16-week-old db/m and db/db mice were obtained from GemPharmatech (Nanjing, China). All animals were housed and maintained according to the standards and procedures approved by the Laboratory Animal Ethics and Welfare Committee of Hebei Medical University (No. IACUC-Hebmu-2021030). AAV9-Ksp-miR-204-5p mimics (Titer: 1×10^{12}) were designed and synthesized by HANBIO (Shanghai, China). db/db mice were randomly divided into three groups (n=6) at 16 weeks of age: (1) db/db, (2) db/db + AAV9-Ksp-miR-204-5p mimics (mimics), (3) db/db + AAV9-Ksp-nonspecific control (CON). We performed tail vein injections of AAV9-Ksp-miR-204-5p mimics and AAV9-Ksp-CON (100 ul/mouse) at 16 weeks. Additionally, db/m mice were divided into three groups with the same intervention as above. During treatment, blood glucose levels were measured every two weeks. After completing treatment for six weeks, the mice were euthanized, and tissues and plasma were rapidly obtained.

Biochemical Analysis

Urine samples were collected for 24h from each mouse placed in metabolic cages. Serum creatinine (Scr), blood urea nitrogen (BUN), and urinary albumin excretion rate (UAE) were quantified using enzyme-linked immunosorbent assay (ELISA) kits (Njjcbio, Nanjing, China) according to the manufacturer's instructions.

Histology Examination and Immunohistochemistry Staining

The renal tissues were fixed using paraformaldehyde (4%) overnight and subsequently embedded using paraffin. Paraffin-embedded tissue sections (2 um) were stained with periodic acid-Schiff (PAS) and Masson's trichrome stain. For immunohistochemistry staining, 4 μm thick paraffin sections were incubated with primary antibodies for fibronectin (1:500), LC3 (1:400), ATG5 (1:600), Nrf2 (1:400), Keap1 (1:200), Nox4 (1:500), and 8-OHdG (1:400). Then, sections were incubated with biotinylated secondary antibody and horseradish peroxidase-conjugated streptavidin. The labeling was visualized with 3.3-dimethylbenzidine. The quantitative analysis of positive staining was performed using ImageJ software (NIH).

Cell Culture and Transfection

Human proximal tubular cells (HK-2) obtained from the American Type Culture Collection (ATCC) were cultured in Roswell Park Memorial Institute (RPMI) 1640 medium supplemented with fetal bovine serum (FBS, 10%) and antibiotic/antimycotic solution (1%) at 37 °C in an incubator with 5% CO2. Before the experiments, when the cells reached 70–80% confluence, they were deprived of serum for 12 h. HK-2 cells were cultured with normal glucose (NG,

5.6 mmol) or high glucose (HG, 30 mmol/L) concentrations in a serum-free medium for different periods. NG plus mannitol (M, 24.4 mM mmol) was used as an anosmatic control. MiR-204-5p mimics, miR-204-5p inhibitor, and siATG5 were transfected into HG-treated HK-2 cells. All transfections were performed with Lipofectamine® 3000 (Invitrogen, Carlsbad, CA, USA) according to the manufacturer's instructions. HK-2 cells were pretreated with Tert-Butylhydroquinone (TBHQ, 30 nM), ML385 (20 uM), or 3-methyladenine (3-MA, 5 mM).

Western Blot Assay

Western blotting was applied as previously described.[26] Proteins from cultured cells and the renal cortex were isolated using a radioimmunoprecipitation assay (RIPA) buffer. The ladders were obtained from Proteintech (Cat No.PL00001) and Supersbrilliant® (ZS-PR24002). The semi-dry blotting protein transfer system of Trans-Blot Turbo and Trans-Blot SD Cell systems (Bio-Rad) were used in the protein transfer process. After blocking nonspecific binding with 5% skim milk, the membranes were incubated with primary antibodies against fibronectin (1:1500), collagen I (1:500), LC3 (1:500), Nrf2 (1:500), Keap1 (1:2000), Nox4 (1;1000), HO-1 (1:1500), ATG5 (1:1000), P62 (1:1000), β-actin (1:1000), GAPDH (1:2000), and Histone H3 (1:1000) for 12 hours at 4 °C followed by horseradish peroxidase-conjugated anti-mouse IgG or horseradish peroxidase-conjugated anti-rabbit IgG. Target proteins were visualized using the chemiluminescent Amersham Imager 600 (Thermo Fisher Scientific) or Tanon 4800. Densitometry was performed using the ImageJ software (National Institutes of Health).

Quantitative Real-time PCR (qRT-PCR)

Total RNA was extracted from HK-2 cells or kidney tissues using TRIzol reagent (Invitrogen, US) according to the manufacturer's instructions. qRT-PCR was performed with SYBR Premix Ex Taq TM II (Takara, Dalian, China) using an Agilent Mx3000P qPCR System (Agilent, CA, USA). The primers for PCR were obtained from Sangon Biotech Co., Ltd. (Shanghai, China) and are listed in Table 1. The relative quantification was performed by determining the $2^{-\Delta\Delta Ct}$ values with U6 and GAPDH as the internal references for miRNA and mRNAs, respectively.

Immunofluorescence Assay

For immunofluorescence analysis, the HK-2 cells were permeabilized using 0.1% Triton X-100 and blocked with 5% goat serum solution, and the cells were incubated overnight with primary antibodies of LC3 (1:400), fibronectin (FN) (1:500), ATG5 (1:800) and Keap1 (1:500) at 4 °C. Then, fluorescein isothiocyanate (FITC)-conjugated goat anti-mouse IgG or CoraLite594-conjugated goat anti-rabbit IgG was added onto the cells and placed in a 37 °C thermostat for 1h.

Table 1 Sequences of Primers Used for RT-qPCR

Gene	Primers	Sequences
H-miR-204-5p	Forward	5′-CTGTCACTCGAGCTGCTGGAATG-3′
	Reverse	5′-CTTGTACCCTCCCAGCGTTT-3′
H-U6	Forward	5′-GCTTCGGCACATA-3′
	Reverse	5′-ATGGAACGCTTCACGA-3′
H-Keap1	Forward	5′- TGCTCAACCGCTTGCTGTATGC −3′
	Reverse	5′- TCATCCGCCACTCATTCCTCTCC −3′
H-Fibronectin	Forward	5′-GCCATTTGCTCCTGCA-3′
	Reverse	5′-CAATTGGGCAATTAACATTA-3′
GADPH	Forward	5′-ATCACTGCCACCCAGAAGAC-3′
	Reverse	5′-TTTCTAGACGGCAGGTCAGG-3′
M-miR-204-5p	Forward	5′-ACACTCCAGCTGGGTTCCCTTTG-3′
	Reverse	5′-CTCAACTGGTGTCGTGGAGTCGG-3′
M-U6	Forward	5′- CGCTTCACGAATTTGCGTGTCAT −3′
	Reverse	5′- GCTTCGGCAGCACATATACTAAAAT-3′

The cells were sealed with glycerine containing 4′,6-diamidino-2-phenylindole (DAPI) (Invitrogen, Carlsbad, CA, USA). The images were captured using a confocal microscope (Leica™ TCS SP8).

Fluorescence in situ Hybridization (FISH)

FISH was performed according to the manufacturer's instructions. The kidney sections from mice were deparaffinized and permeabilized with 0.2% Triton X-100. The sections were then hybridized with miR-204-5p probes (Gene Pharma, Suzhou, China) in a hybridization buffer for 15 h. Images were captured using a confocal microscope (Leica, Germany).

Measurement of ROS

MitoSox Red (Invitrogen, Carlsbad, CA, USA) was used to examine the level of mitochondrial reactive oxygen species (ROS) of HK-2 cells. Then, HK-2 cells were treated with MitoSox Red reagent (5μM) at 37°C for 15 min in the dark. The cells were photographed using a confocal microscope (Leica, Germany).

ELISA Assay

ELISA kits were used to examine the levels of fibronectin in the supernatant of HK-2 cells and 8-OHdG in urine, according to the manufacturer's instructions.

Statistical Analyses

Statistical analyses were performed using the GraphPad Prism 8.3.0 (GraphPad Software Inc.). Data were presented as mean ± standard error of mean (SEM). Student's *t*-test was used to compare differences between the two groups. One-way ANOVA was performed for multiple group comparison. Shapiro–Wilk test was performed for normality analysis by using SPSS 22.0 software. $p < 0.05$ was considered statistically significant.

Results

MiR-204-5p Alleviates Kidney Injury in Db/Db Mice

As shown in Figure 1A, the expression of miR-204-5p in diabetic kidneys was significantly reduced compared to that in db/m mice by qRT-PCR. Fluorescence in situ hybridization (FISH) also indicated that miR-204-5p expression was lower in db/db mice than that of db/m mice and mainly expressed in the renal tubule (Figure 1B). To determine the role of miR-204-5p on diabetic renal injury, an AAV9-Ksp-miR-204-5p mimics vector was delivered into the kidneys of mice. MiR-204-5p mimics significantly enhanced miR-204-5p expression in db/db and db/m mice (Figure 1A and B). Mesangial area increased in db/db mice compared with db/m mice. Treatment with miR-204-5p mimics restrained mesangial expansion in db/db mice (Figure 1C and D). Masson's trichrome staining was a sign for evaluating the severity of renal fibrosis in diabetic mice. Compared with db/m mice, the distribution of Masson's trichrome-positive areas was elevated in db/db mice, whereas this change could be inhibited by miR-204-5p mimics (Figure 1C and E). Moreover, the expression of fibronectin in renal tissue was increased, and miR-204-5p mimics obviously retarded this alteration in db/db mice compared with db/m mice (Figure 1C). Furthermore, Western blot showed that miR-204-5p mimics reduced the high expression of fibronectin and collagen I in the renal tissue of db/db mice (Figure 1F). Compared with db/m mice, blood glucose was higher in all db/db mice, whereas increasing the expression of miR-204-5p did not affect blood glucose levels (Figure 1G). To confirm renal function, we measured serum creatinine (Scr), blood urea nitrogen (BUN), 24h urine albumin excretion (UAE), and urine albumin/creatinine ratio (UACR). Renal function was damaged in db/db mice, and treatment with the miR-204-5p mimics alleviated this damage (Figure 1H–K). Therefore, these results indicate that miR-204-5p protects against the progression of diabetic kidney disease.

MiR-204-5p Restores Renal Autophagy in Db/Db Mice

Maintaining the homeostasis of autophagy is essential for normal renal function, and renal autophagy dysregulation is intimately related to the progression of DKD.[27] Compared with db/m mice, the expression of LC3 and ATG5 was reduced in db/db mice, and these changes were reversed by miR-204-5p mimics (Figure 2A–C). In addition, Western blot indicated

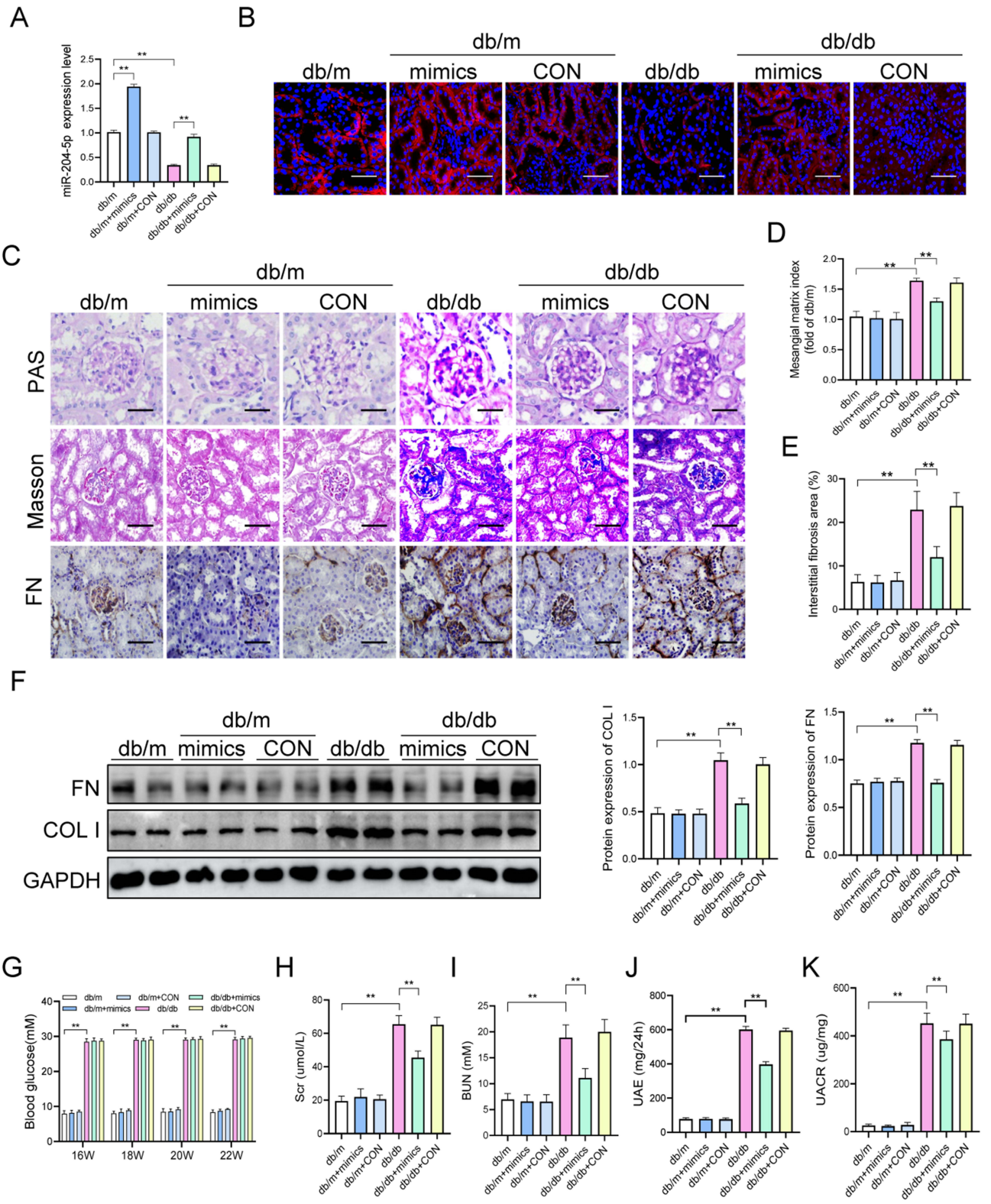

Figure 1 MiR-204-5p overexpression alleviates kidney injury in db/db mice. (**A**) qRT-PCR was performed to detect miR-204-5p expression in the kidneys. (**B**) MiR-204-5p expression detected by FISH. (**C**) PAS staining (scale bar = 25μm), Masson's staining, and immunohistochemical staining of fibronectin were performed to investigate histopathological analysis of the kidneys (scale bar = 50μm). (**D** and **E**) Mesangial area of glomeruli and glomerular volume were measured. (**F**) Western blot analysis of fibronectin (FN) and collagen I (COL). (**I**) level in different groups. (**G**) Blood glucose, (**H**) Serum creatinine (Scr), (**I**) Blood urea nitrogen (BUN), (**J**) urine albumin excretion (UAE), and (**K**) Albumin-to-creatinine ratio (UACR) were measured. $^{**}p < 0.01$, ns: no significance.

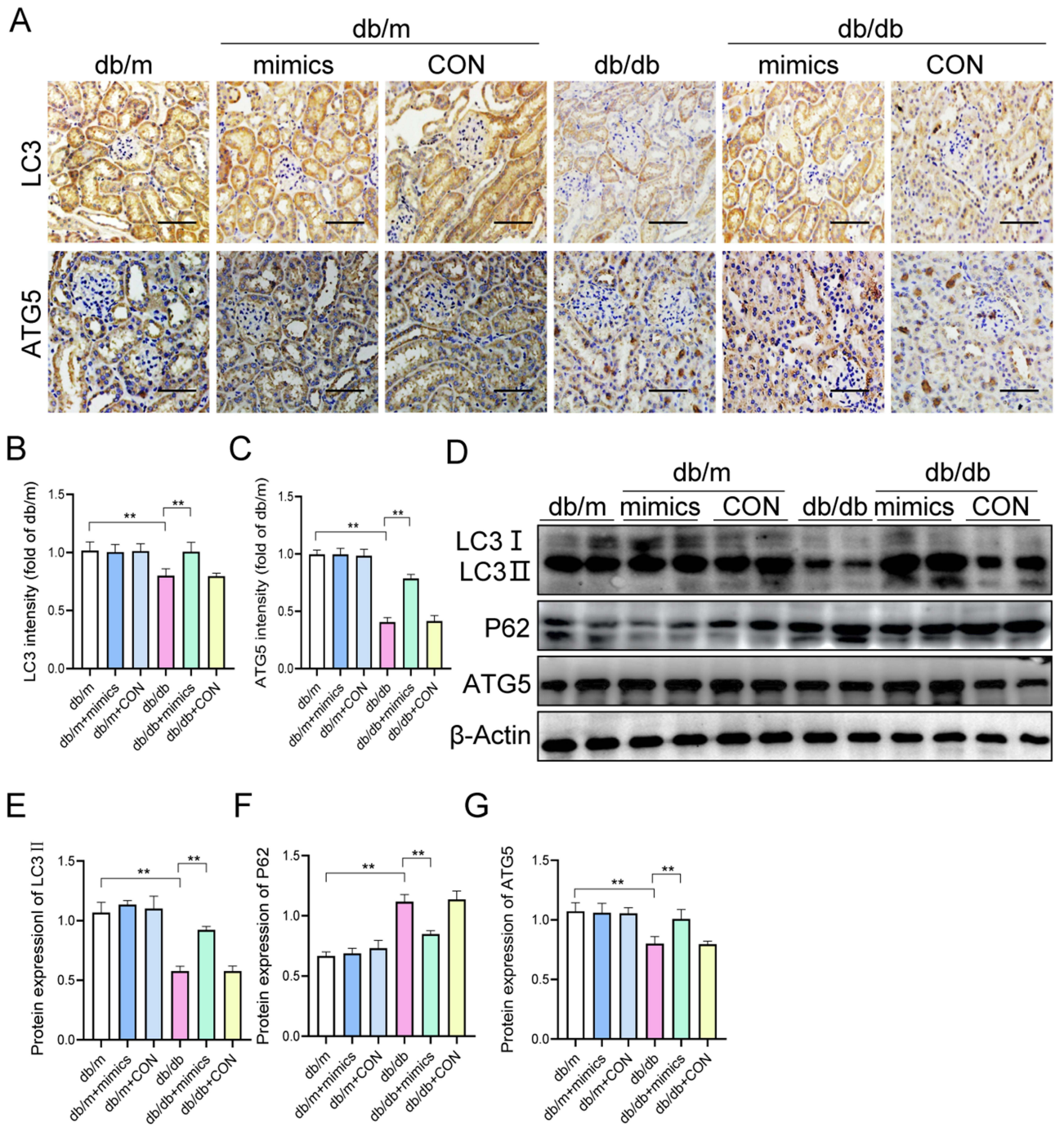

Figure 2 MiR-204-5p overexpression restores renal autophagy in db/db mice. (**A**) Immunohistochemical staining of LC3 and ATG5 in paraffin-embedded renal tissues from different groups (scale bar = 50μm). (**B** and **C**) Quantification of LC3 and ATG5 expression in renal tissues. (**D**–**G**). Western blot analysis of LC3, P62, and ATG5 level in different groups. $^{**}p < 0.01$.

that the expression of LC3 and ATG5 was restrained, and P62 expression was increased in diabetic kidneys compared with the control group (Figure 2D–G). These alterations were abolished by miR-204-5p mimics. (Figure 2D–G). These data demonstrate that increasing the expression of miR-204-5p has positive regulation on autophagy.

MiR-204-5p Reduces Oxidative Stress in Db/Db Mice

Nox4 was involved in the production of ROS in the kidneys during the progression of diabetic kidney diseases.[28] Thus, we examined the expression of Nox4 using Western blot and immunohistochemistry. Compared with db/m mice, the

expression of Nox4 was up-regulated in renal tissues of db/db mice, and the abnormal expression could be inhibited by miR-204-5p mimics (Figure 3A–C). In addition, miR-204-5p mimics treatment significantly suppressed the expression of 8-OHdG, a sign of oxidative stress, in diabetic kidneys (Figure 3B and D). Moreover, the urinary excretion of 8-OHdG in db/db mice was obviously reduced by miR-204-5p mimics treatment (Figure 3E).

MiR-204-5p Attenuates Keap1 Expression and Enhances Nrf2 Expression in Diabetic Kidneys

The Kelch-like ECH-associated protein 1 (Keap1)-nuclear factor erythroid 2-related factor 2 (Nrf2) pathway is a classical antioxidant stress pathway[29] and plays a vital role in diabetic kidney diseases.[30] The results of

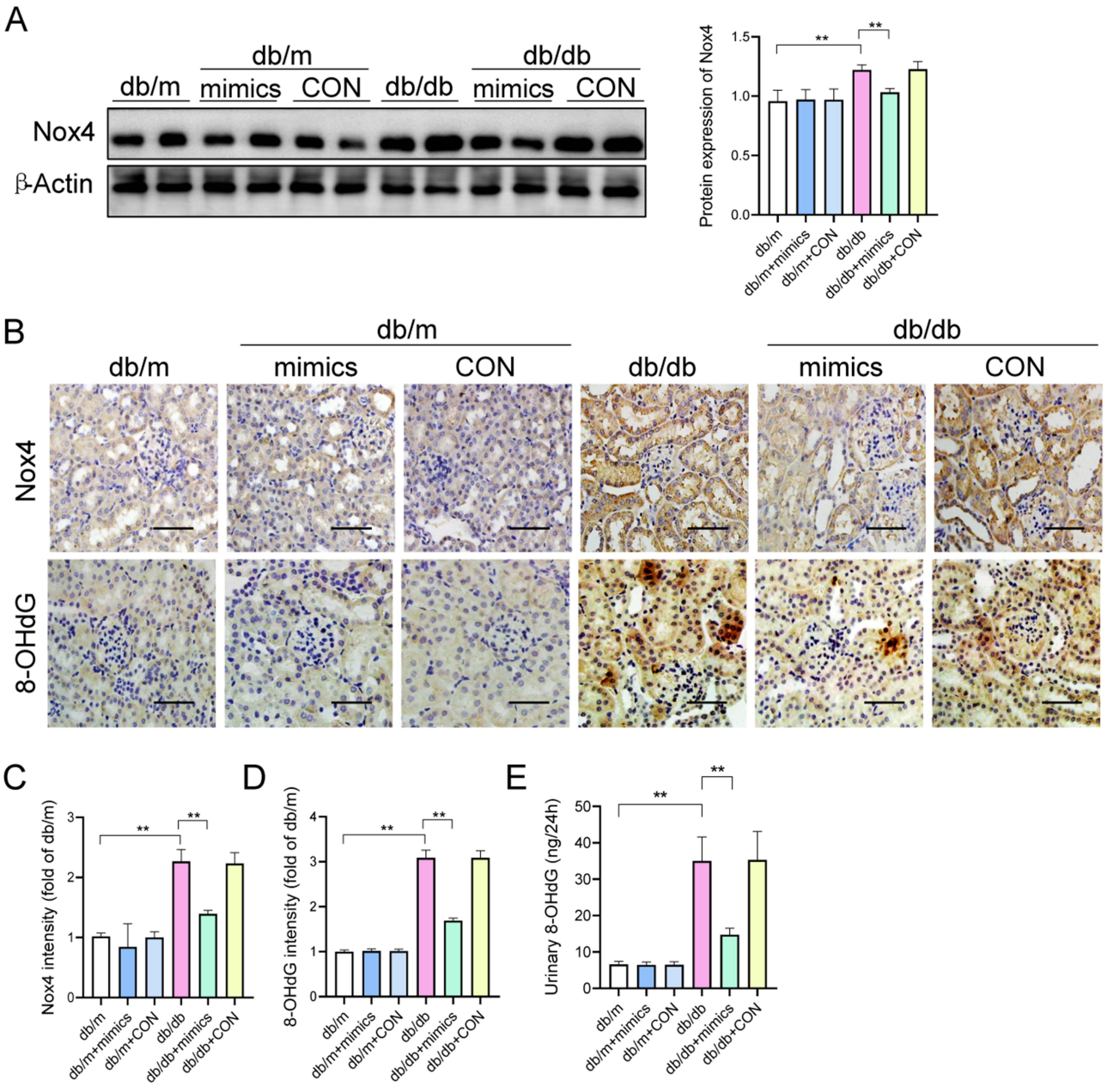

Figure 3 MiR-204-5p overexpression reduces oxidative stress in db/db mice. (**A**) Western blot analysis of Nox4 level in different groups. (**B**) Immunohistochemical staining of Nox4 and 8-OHdG in paraffin-embedded renal tissues from different groups (scale bar = 50μm). (**C** and **D**) Quantification of Nox4 and 8-OHdG expression in renal tissues. E. 24-hour urinary 8-OHdG excretion was detected using ELISA. $^{**}p < 0.01$.

immunohistochemical staining showed that the Keap1 expression was increased and Nrf2 expression was decreased in the renal tubule and glomeruli of db/db mice compared with db/m mice, and delivery of miR-204-5p mimics could arrest these alterations (Figure 4A–C). In addition, Western blot indicated that the Keap1 expression was significantly increased and the expression of Nrf2 and HO-1 was inhibited in db/db mice compared with db/m mice. However, the abnormal expression of these proteins was inhibited by the treatment of miR-204-5p mimics (Figure 4D and E).

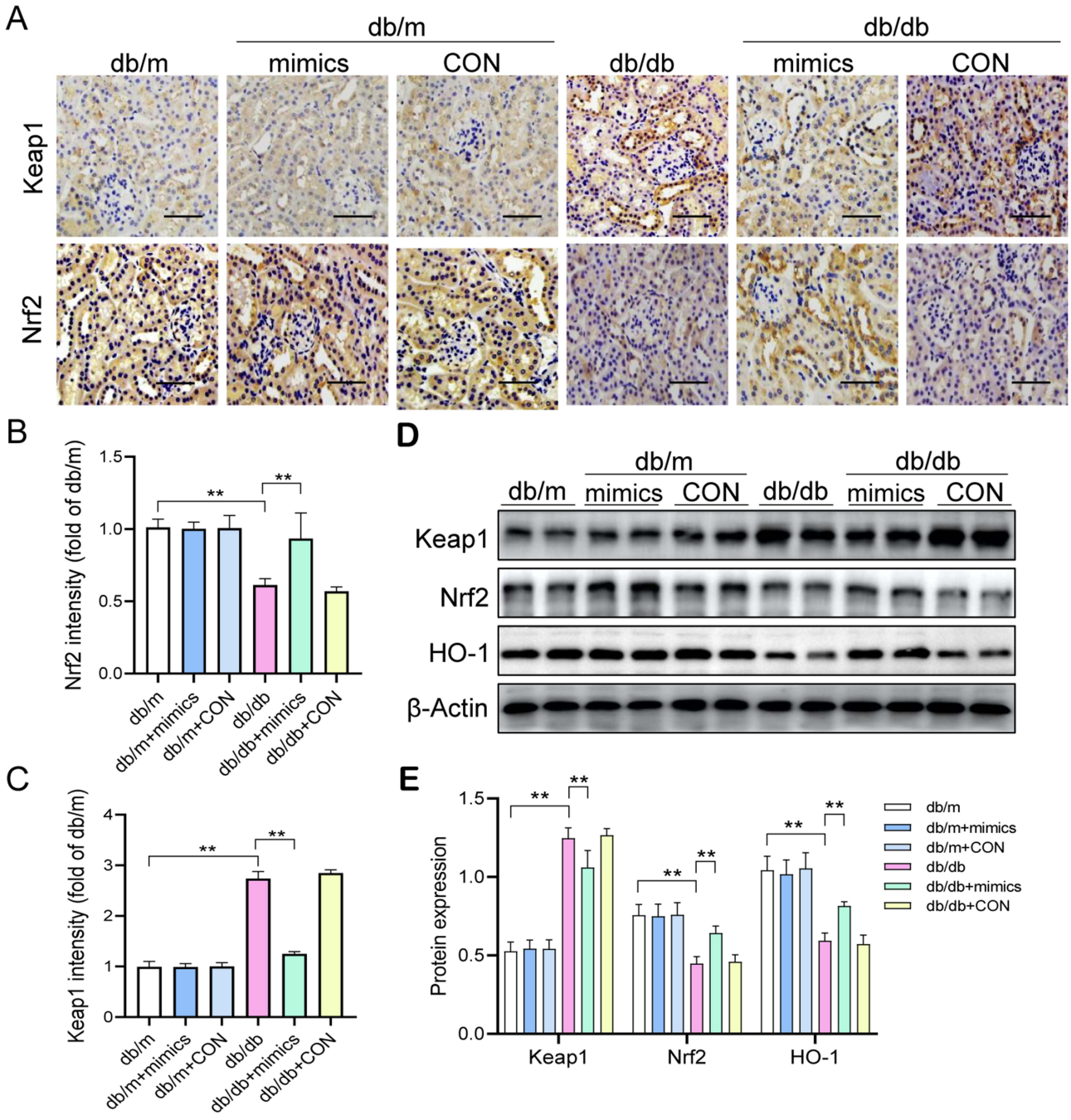

Figure 4 MiR-204-5p overexpression attenuates Keap1 expression and enhances Nrf2 expression in diabetic kidneys. (**A**) Immunohistochemical staining of Keap1 and Nrf2 in paraffin-embedded renal tissues from different groups (scale bar = 50μm). (**B** and **C**) Quantification of Keap1 and Nrf2 expression in renal tissues. (**D** and **E**) Western blot analysis of Keap1 and Nrf2 level in different groups. $^{**}p < 0.01$.

MiR-204-5p Inhibitor Enhances Fibronectin and Collagen I Expressions and Reduces Autophagy in HG-Treated HK-2 Cells

As shown in Figure 5A, the expression of miR-204-5p was suppressed in HG-treated HK-2 cells compared with the NG group. To investigate the effect of miR-204-5p on autophagy and the expression of fibronectin and collagen I, miR-204-5p inhibitor or miRNA control was transfected into HK-2 cells. Transfection of miR-204-5p inhibitor further inhibited the expression of miR-204-5p in HK-2 cells exposed to HG (Figure 5A and B). In addition, FISH demonstrated that miR-204-5p expressed in the cytoplasm and nucleus of HK-2 cells (Figure 5B). Western blot showed that miR-204-5p inhibitor enhanced the expression of fibronectin and collagen I in HG-induced HK-2 cells (Figure 5C). The immunofluorescence results of fibronectin were consistent with those of Western blot (Figure 5D). Moreover, the increased concentration of fibronectin was enhanced by miR-204-5p inhibitor in the culture media of HK-2 cells exposed to HG (Figure 5E). Furthermore, miR-204-5p inhibitor reduced the expression of the LC3 and ATG5 and enhanced P62 expression in HG-treated HK-2 cells (Figure 5F). Immunofluorescent further confirmed that miR-204-5p inhibitor exacerbated the HG-induced LC3 reduction (Figure 5G).

MiR-204-5p Overexpression Ameliorates HG-Induced Fibronectin and Collagen I Expressions by Restoring Autophagy in HK-2 Cells

Increasing miR-204-5p expression by transfecting miR-204-5p mimics could increase the expression of LC3 and ATG5 and decrease the expression of P62 in HK-2 cells exposed to HG (Figure 6A). The immunofluorescence results of LC3 were consistent with those of Western blot (Figure 6B). However, the effects of miR-204-5p mimics on autophagy were abolished by autophagy inhibitor 3-MA treatment (Figure 6A and B). In addition, miR-204-5p mimics decreased the expression of fibronectin and collagen I in HG-induced HK-2 cells (Figure 6C and D). The expression of fibronectin was detected by immunofluorescent staining, and the result was consistent with those of Western blot (Figure 6E). However, the ability of miR-204-5p mimics to correct the levels of fibronectin and collagen I was obviously prevented in the presence of 3-MA (Figure 6C–E). As shown in Figure 6F, the increased concentration of fibronectin was reduced by transfecting of miR-204-5p mimics in the culture media of HK-2 cells exposed to HG, while 3-MA reversed this change caused by miR-204-5p mimics. Moreover, miR-204-5p mimics inhibited HG-induced fibronectin mRNA expression, and 3-MA abolished the effects of miR-204-5p mimics on fibronectin mRNA expression (Figure 6G).

Next, the expression of ATG5 was restrained using ATG5 siRNA to determine further the relationship between autophagy and fibronectin and collagen I expression in HK-2 cells exposed to HG. As shown in Figure 6H and I, ATG5 silencing eliminated the effect of miR-204-5p mimics on autophagy. The immunofluorescence results of LC3 and ATG5 were consistent with those of the Western blot (Figure 6J). In addition, the role of miR-204-5p mimics on the expression of fibronectin and collagen I was abolished by ATG5 knockdown in HG-treated HK-2 cells (Figure 6K). Therefore, these results reveal that miR-204-5p may reduce fibronectin and collagen I expression by restoring autophagy.

MiR-204-5p Enhances Autophagy by Upregulation of Nrf2 in HG-Induced HK-2 Cells

Transfection of miR-204-5p inhibitor significantly decreased the total Nrf2 and nuclear-Nrf2 proteins abundance in HK-2 cells exposed to HG, while activation of Nrf2 by TBHQ reversed these alterations induced by miR-204-5p inhibitor (Figure 7A). In addition, the impact of autophagy inhibition brought by miR-204-5p inhibitor was reversed by TBHQ in HG-treated HK-2 cells (Figure 7B and C). Moreover, TBHQ abated the effect of miR-204-5p inhibitor on the expression of fibronectin and collagen I (Figure 7D).

In HG-induced HK-2 cells, the transfection of miR-204-5p mimics increased the expression of total-Nrf2 and nuclear-Nrf2, and these changes were reversed by ML385, which inhibited Nrf2 expression (Figure 7E). In addition, the induction of autophagy by miR-204-5p mimics treatment was inhibited by ML385 in HG-treated HK-2 cells (Figure 7F and G). Moreover, ML385 arrested the effect of miR-204-5p mimics on fibronectin and collagen I expression (Figure 7H). Immunofluorescence results of LC3 and fibronectin were consistent with those of the Western blot (Figure 7I). Furthermore, the production of ROS was detected by MitoSOX Red. We found that HG-induced ROS production was reduced by transfection of miR-204-5p mimics in HK-2 cells. However, the effect of miR-

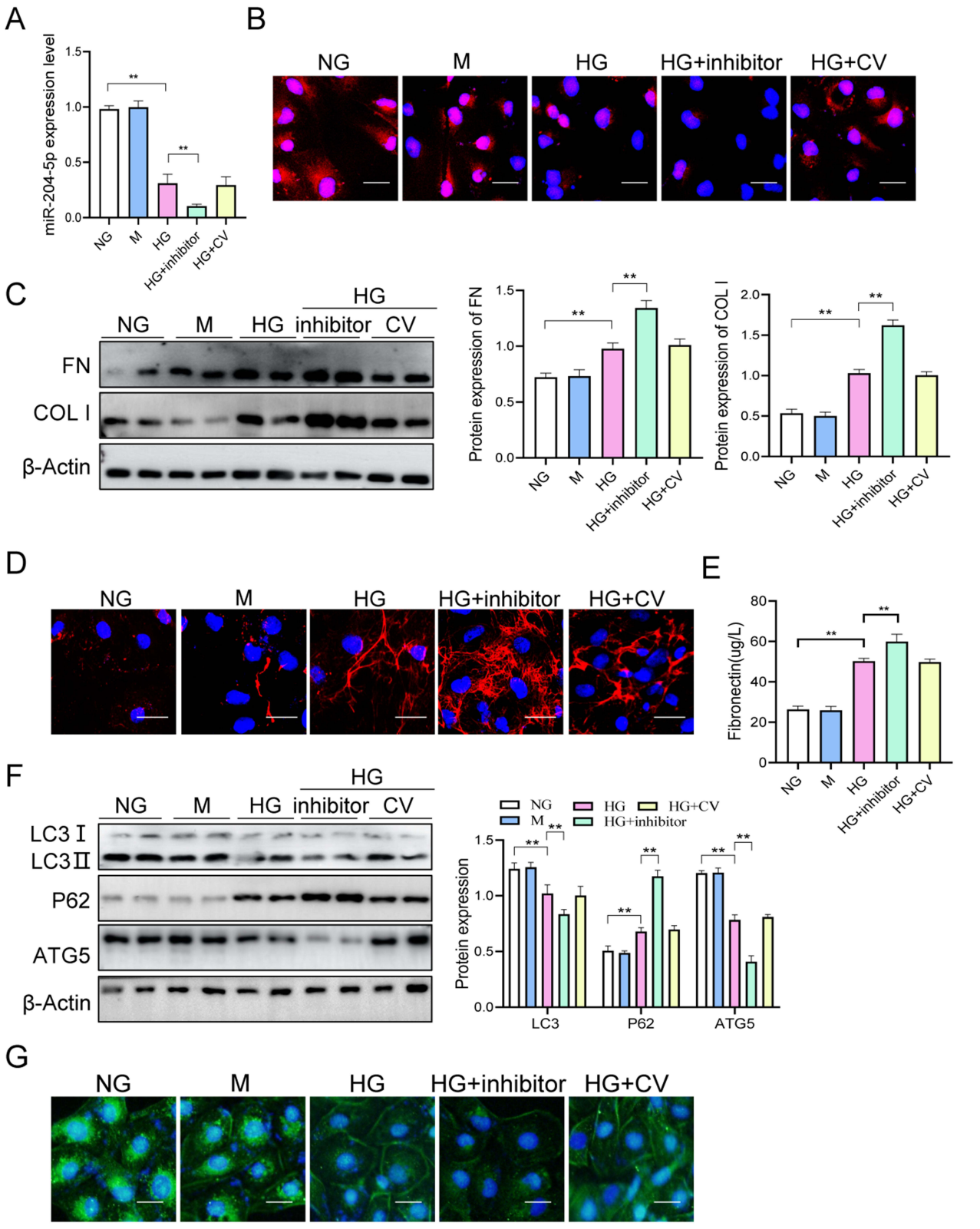

Figure 5 MiR-204-5p inhibitor enhances fibronectin and collagen I expressions and reduces autophagy in HG-treated HK-2 cells. (**A**) The expression of miR-204-5p was measured using qRT-PCR. (**B**) FISH was performed to detect the expression of miR-204-5p. (**C**) The protein levels of FN and COL I were measured using Western blot analysis. (**D**) The level of FN was measured using immunofluorescence (scale bar = 25μm). (**E**) The concentration of FN in the culture media of HK-2 cells were evaluated using ELISA. (**F**) The protein levels of LC3, P62, and ATG5 were measured using Western blot analysis. (**G**) The level of LC3 was measured using immunofluorescence (scale bar = 25μm). $^{**}p < 0.01$.

https://doi.org/10.2147/DMSO.S441082 DovePress

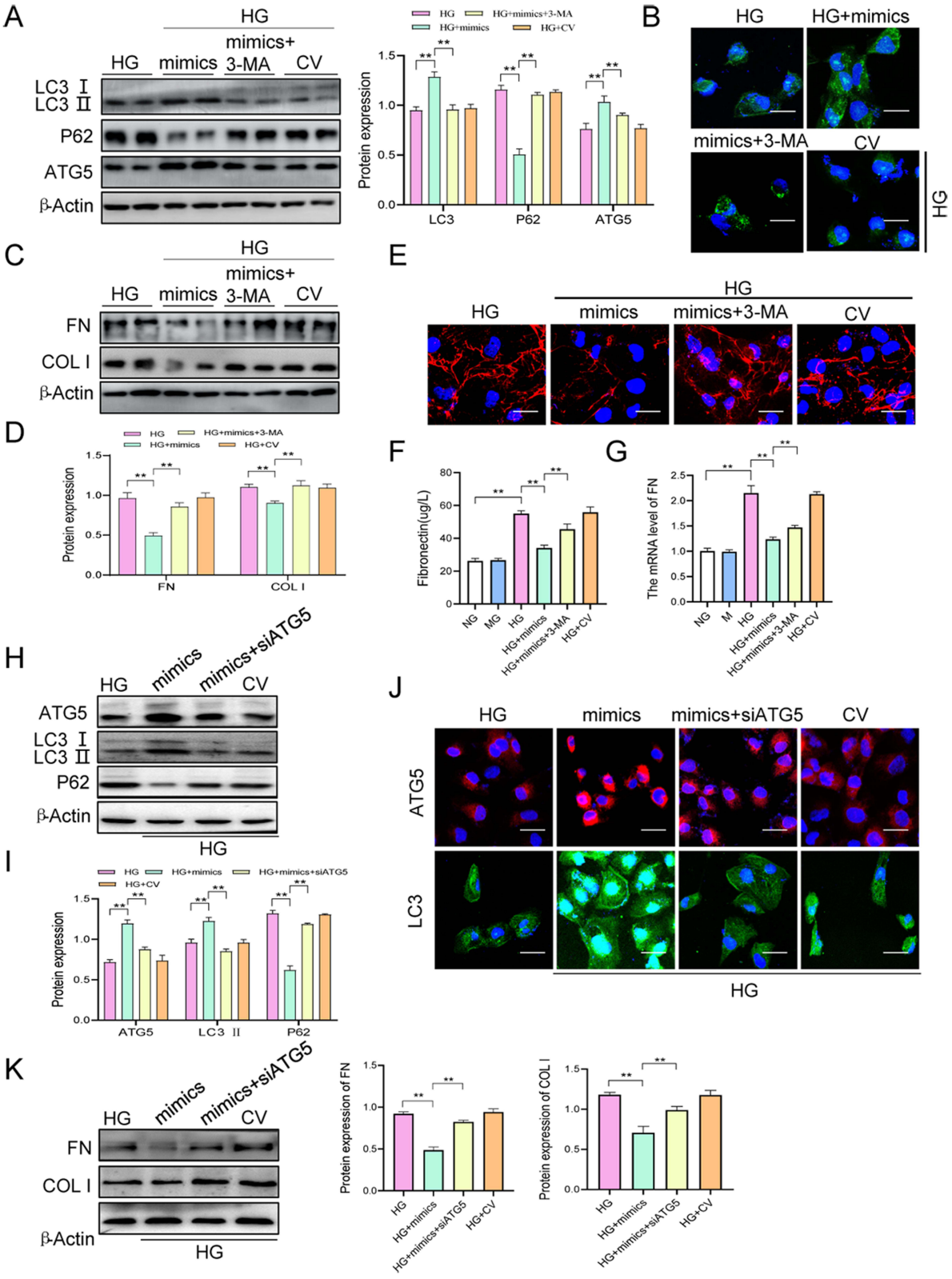

Figure 6 MiR-204-5p overexpression ameliorates HG-induced fibronectin and collagen I expressions by restoring autophagy in HK-2 cells. (**A**) The expression of LC3, P62, and ATG5 was measured using Western blot analysis. (**B**). Immunofluorescence was performed to detect the expression of LC3 (scale bar = 25μm). (**C** and **D**). The expression of FN and COL I was measured using Western blot analysis. (**E**). Immunofluorescence was performed to detect the expression of FN (scale bar = 25μm). (**F**) The concentrations of FN in the culture media of HK-2 cells were evaluated using ELISA. (**G**) The relative mRNA expression of FN was measured using qRT-PCR. (**H** and **I**). The expression of ATG5, LC3, and P62 was measured using Western blot analysis. (**J**). Immunofluorescence was performed to detect the expression of ATG5 and LC3 (scale bar = 25μm). (**K**) The expression of FN and COL I was measured using Western blot analysis. $^{**}p < 0.01$.

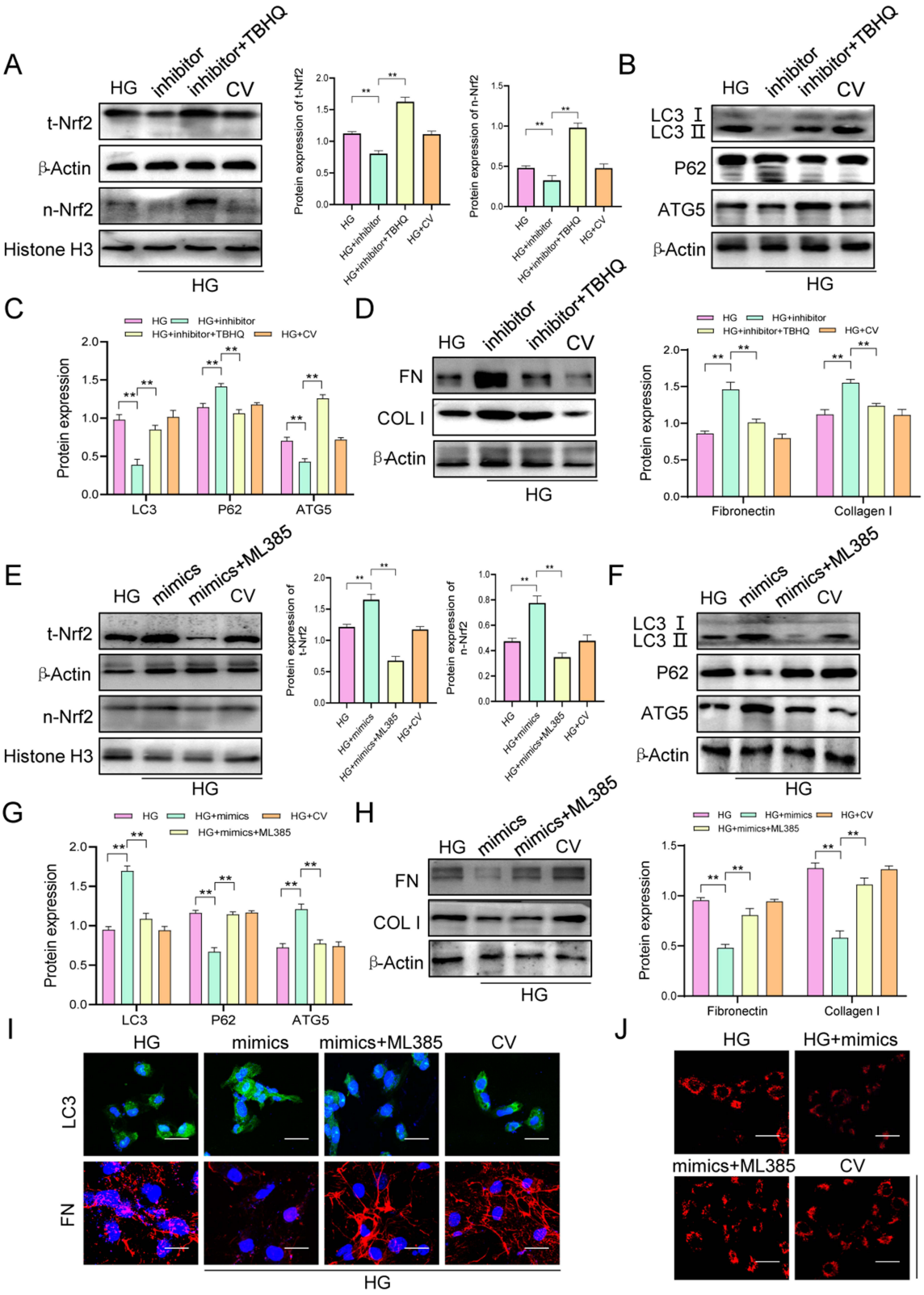

Figure 7 MiR-204-5p alleviates HG-induced fibrosis through Nrf2 autophagy in HK-2 cells. (**A**) The expression of total-Nrf2 and nuclear-Nrf2 was measured using Western blot analysis. (**B** and **C**). The expression of LC3, P62, and ATG5 was measured using Western blot analysis. (**D**) The expression of FN and COL I was measured using Western blot analysis. (**E**) The expression of total-Nrf2 and nuclear-Nrf2 was measured using Western blot analysis. (**F** and **G**). The expression of LC3, P62, and ATG5 was measured using Western blot analysis. (**H**) The expression of FN and COL I was measured using Western blot analysis. (**I**) Immunofluorescence was performed to detect the expression of LC3 and fibronectin (scale bar = 25μm). (**J**) MitoSOX RED was performed to investigate the ROS levels in the mitochondria of HK-2 cells (scale bar = 10μm). $^{**}p < 0.01$.

https://doi.org/10.2147/DMSO.S441082 DovePress

204-5p mimics on ROS production was retarded by ML385 (Figure 7J). These results demonstrated that miR-204-5p may induce autophagy by upregulating Nrf2 in HG-treated HK-2 cells.

MiR-204-5p Regulates Nrf2 by Sponging Keap1 mRNA

We used the software of Starbase to seek for the target mRNAs interacting with miR-204-5p. Notably, the mRNA of Keap1 was a predicted target mRNA of miR-204-5p (Figure 8A). The direct interaction between miR-204-5p and Keap1 was determined by dual-luciferase reporter assay. The transient co-transfection of miR-204-5p mimics and the wild-type Keap1 luciferase reporter in HK-2 cells significantly reduced the luciferase activity (Figure 8B). However, the co-transfection of miR-204-5p mimics and the mutant-type Keap1 luciferase reporter has no effect on the luciferase activity (Figure 8B). In addition, the mRNA expression of Keap1 was inhibited by miR-204-5p mimics in HK-2 cells exposed to HG (Figure 8C). Moreover, we detected the protein expression of Keap1, Nrf2, and HO-1 using Western blot. The results showed that transfection of miR-204-5p mimics reduced the protein expression of Keap1 and enhanced the expression of Nrf2 and HO-1 in HG-induced HK-2 cells (Figure 8D and E). Immunofluorescence results indicated that miR-204-5p mimics inhibited the increasing protein expression of Keap1 in the HG group in HK-2 cells (Figure 8F). Furthermore,

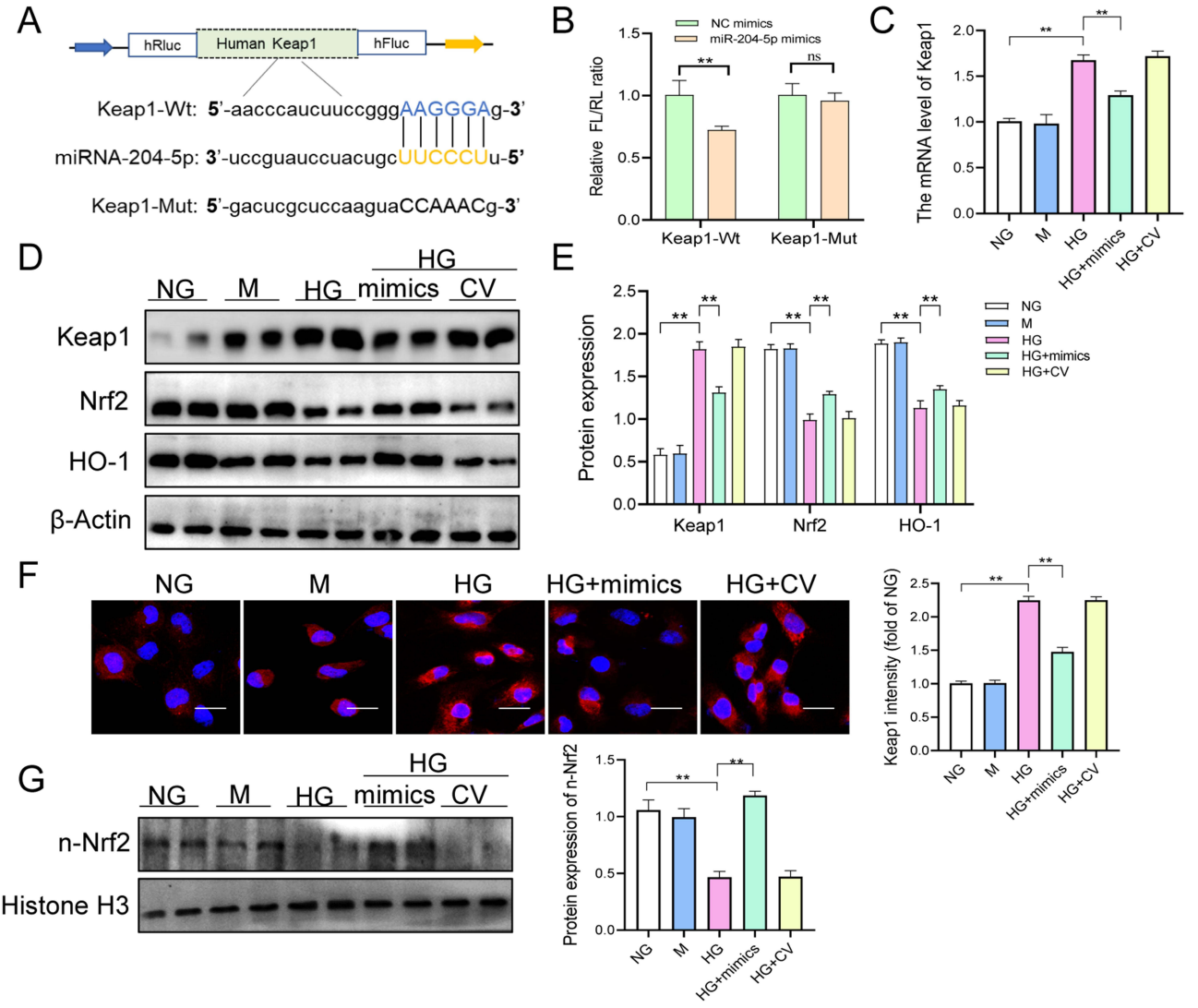

Figure 8 MiR-204-5p directly targeted keap1 mRNA. (**A**) The binding site of miR-204-5p and Keap1. (**B**) Dual-luciferase reporter. (**C**) The expression of Keap1 mRNA was measured using qRT-PCR. (**D** and **E**). The expression of Keap1, Nrf2, and HO-1 was measured using Western blot analysis. (**F**) Immunofluorescence was performed to detect the expression of Keap1 (scale bar = 25μm). (**G**) The expression of nuclear-Nrf2 was measured using Western blot analysis. $^{**}p < 0.01$.

miR-204-5p mimics increased the nuclear-Nrf2 expression in HG-treated HK-2 cells (Figure 8G). In summary, we speculated that miR-204-5p might affect the expression of Keap1 through competitively binding the mRNA of Keap1 in HK-2 cells.

Discussion

In this study, we aimed to confirm the effects and underlying molecular mechanisms of miR-204-5p in DKD. The expression of miR-204-5p was decreased in the kidneys of db/db mice. We confirmed that the miR-204-5p mimics obviously ameliorated renal injury and oxidative stress and restored autophagy in db/db mice. Notably, we provided evidence that miR-204-5p mimics inhibited the expression of fibronectin and collagen I by enhancing autophagy via regulating the Keap1/Nrf2 signal pathway in HK-2 cells exposed to HG.

Collecting evidence shows that the accumulation of fibrosis-related factors, fibronectin, and collagen I, is one of the characteristic pathological changes in DKD, which can cause renal fibrosis.[31] In diabetic renal tubules, interstitial fibrosis and atrophy are the common features of pathogenic change, which eventually lead to renal dysfunction.[32] Previous studies have reported that HG promoted HK-2 cells elevated expression levels of fibronectin and collagen I proteins.[33] Our current study showed that HG significantly induced the expression of fibronectin and collagen I in HK-2 cells. However, the effects of HG on HK-2 cells fibronectin and collagen I expression were mitigated by miR-204-5p overexpression or aggravated by miR-204-5p knockdown. In addition, delivery of miR-204-5p mimics improved renal function, attenuated mesangial expansion, fibronectin, collagen I expressions, and oxidative stress in diabetic mice. These findings reveal that miR-204-5p protects against the progression of DKD by alleviate renal fibrosis.

Autophagy is required to reprogram somatic cells to a pluripotent state and maintain pluripotency.[34] Adaptive autophagy exerts a protective effect on the kidneys, and autophagy impairment participates in the pathogenesis of DKD.[35] Recent research has indicated that the restoration of autophagy inhibits the progression of fibrosis and the aggravation of DKD.[36] Previous study has demonstrated that miR-204-5p overexpression restore TGF-β1 induced impairment of autophagy in human tenon capsule fibroblasts (HTFs).[37] Our results demonstrated that miR-204-5p overexpression corrects the altered expression of LC3, P62, and ATG5 in vitro and in vivo. However, the anti-fibrosis effects of miR-204-5p are halted in the presence of the autophagy inhibitor 3-MA or ATG5 siRNA. These results confirm that the beneficial regulation of autophagy by miR-204-5p contributes obviously to its anti-fibrosis-related factors production functions.

Oxidative stress with accumulated reactive oxygen species (ROS) production is a vital pathogenic factor in the progression of DKD.[38] Increased ROS mediated HG-induced fibronectin and collagen I expression in HK-2 cells.[39] One of the sources of ROS induced by diabetic is the increased NADPH oxidase activation, especially Nox4 subtype, contributing to increased oxidative stress in renal cells.[40] Previous study has revealed that miR-204 plays a vital role in the oxidative stress process through G protein signaling 12 (RGS12) signal pathway.[41] Collecting evidence has demonstrated that Nrf2 is an essential regulator of cellular anti-oxidative stress and a pivotal factor of DKD.[42] Nrf2 activation could suppress HG-induced oxidative stress and fibrotic responses in human renal proximal tubular (HK11) cells.[43] In addition, Nrf2 beneficially regulates multiple cellular processes that are critically involved in DKD, such as autophagy[44] and apoptosis.[45] Consistent with this result, the HG-induced generation of the ROS was decreased by miR-204-5p overexpression in HK-2 cells. Meanwhile, miR-204-5p overexpression promoted Nrf2 activation in HK-2 cells exposed to HG. Besides, Nrf2 inhibitor ML385 could reverse the effect of miR-204-5p mimics on HG-induced autophagy and fibrotic responses protein fibronectin and collagen I expression in HK-2 cells, showing the effect of ROS on autophagy and fibrotic responses under HG conditions. Moreover, we also found miR-204-5p overexpression could suppress the level of renal oxidative stress in diabetic mice. Taken together, these data showed that miR-204-5p overexpression prevents diabetes-induced HK-2 cell autophagy damage and fibrotic responses by reducing ROS production.

It has been reported that the Keap1/Nrf2 pathway participates in regulating several cellular processes, such as fibrosis[46] and autophagy.[44] Under physiological conditions, Nrf2 is produced and degraded, regulated by Keap1 via the pathway of ubiquitination, but under stress conditions, Nrf2 is released from Keap1 and enters the cell nucleus, which transactivates a large number of antioxidants, including HO-1.[47] In addition, inhibition of the level of oxidative stress in

the kidney by regulating the Keap1/Nrf2 pathway can improve the progression of DKD.[48] In this study, we found that miR-204-5p overexpression would reduce the protein level of keap1 while increasing the protein level of Nrf2 and HO-1 in diabetic kidneys or HK-2 cells exposed to HG, indicating that miR-204-5p was found to prevent the diabetes-induced increase of Keap1. However, the underlying molecular mechanism of miR-204-5p in type 1 diabetes mouse models with distinct genetic backgrounds needs to be further elucidated.

Conclusion

In conclusion, our data strongly suggest a protective effect of miR-204-5p against the progression of diabetic renal fibrosis. MiR-204-5p alleviated renal damage via restoring autophagy by regulating the Keap1/Nrf2 pathway in diabetic kidney disease. These results demonstrate that positively modulating miR-204-5p might be a promising therapeutic target for DKD. In summary, the results of this study demonstrate a novel target molecule and some potential mechanisms that may be involved in diabetic kidney injury. Such findings provide a basis for new strategies for the treatment of DKD.

Abbreviations

DKD, diabetic kidney diseases; Nrf2, nuclear factor erythroid 2-related factor 2; Keap1, Kelch-like ECH-associated protein 1; ROS, reactive oxygen species; FISH, fluorescence in situ hybridization; TBHQ, Tertiarybutylhydroquinone; 3-MA, 3-Methyladenine.

Data Sharing Statement

Data supporting the findings of this study are available from the corresponding author upon reasonable request.

Author Contributions

All authors made a significant contribution to the work reported, whether that is in the conception, study design, execution, acquisition of data, analysis and interpretation, or in all these areas; took part in drafting, revising or critically reviewing the article; gave final approval of the version to be published; have agreed on the journal to which the article has been submitted; and agree to be accountable for all aspects of the work.

Funding

This study was supported by grants from the National Natural Science Foundation of China (NO. 81470966), Guiding Local Scientific and Technological Development by the Central Government of China (No. 216Z7703G), and Natural Science Foundation of Hebei Province (No. H2021206144; NO. H2019206179).

Disclosure

The authors declare no conflicts of interest related to the work described in this article.

References

1. Thomas MC, Brownlee M, Susztak K, Sharma K, Jandeleit-Dahm KAM. Diabetic kidney disease. *Nat Rev Dis Primers*. 2015;1:15018. doi:10.1038/nrdp.2015.18
2. Liu ZH. Nephrology in China. *Nat Rev Nephrol*. 2013;9:523–528. doi:10.1038/nrneph.2013.146
3. Collins AJ, Foley RN, Chavers B, et al. US renal data system 2013 annual data report. *Am J Kidney Dis*. 2014;63:A7.
4. Mise K, Hoshino J, Ueno T, et al. Prognostic value of tubulointerstitial Lesions, Urinary N-Acetyl-beta-d-glucosaminidase, and urinary beta2-microglobulin in patients with type 2 diabetes and biopsy-proven diabetic nephropathy. *Clin J Am Soc Nephrol*. 2016;11:593–601. doi:10.2215/CJN.04980515
5. Xu C, Ha X, Yang S, Tian X, Jiang H. Advances in understanding and treating diabetic kidney disease: focus on tubulointerstitial inflammation mechanisms. *Front Endocrinol*. 2023;14:1232790. doi:10.3389/fendo.2023.1232790
6. Xu L, Zhou Y, Wang G, et al. The UDPase ENTPD5 regulates ER stress-associated renal injury by mediating protein N-glycosylation. *Cell Death Dis*. 2023;14:166. doi:10.1038/s41419-023-05685-4
7. Li S, Lin Z, Xiao H, et al. Fyn deficiency inhibits oxidative stress by decreasing c-Cbl-mediated ubiquitination of Sirt1 to attenuate diabetic renal fibrosis. *Metabolism*. 2023;139:155378. doi:10.1016/j.metabol.2022.155378
8. Sharma N, Sistla R, Andugulapati SB. Yohimbine ameliorates liver inflammation and fibrosis by regulating oxidative stress and Wnt/β-catenin pathway. *Phytomedicine*. 2024;123:155182. doi:10.1016/j.phymed.2023.155182

9. Wang F, Sun H, Zuo B, et al. Metformin attenuates renal tubulointerstitial fibrosis via upgrading autophagy in the early stage of diabetic nephropathy. *Sci Rep*. 2021;11:16362. doi:10.1038/s41598-021-95827-5
10. Warren AM, Knudsen ST, Cooper ME. Diabetic nephropathy: an insight into molecular mechanisms and emerging therapies. *Expert Opin Ther Targets*. 2019;23:579–591. doi:10.1080/14728222.2019.1624721
11. Filomeni G, De Zio D, Cecconi F. Oxidative stress and autophagy: the clash between damage and metabolic needs. *Cell Death Differ*. 2015;22:377–388. doi:10.1038/cdd.2014.150
12. Galetaki DM, Cai CL, Bhatia KS, Chin V, Aranda JV, Beharry KD. Biomarkers of growth and carbohydrate metabolism in neonatal rats supplemented with fish oil and/or antioxidants during intermittent hypoxia. *Growth Hormone IGF Res*. 2023;68:101513. doi:10.1016/j.ghir.2022.101513
13. Valko M, Izakovic M, Mazur M, Rhodes CJ, Telser J. Role of oxygen radicals in DNA damage and cancer incidence. *Mol Cell Biochem*. 2004;266:37–56. doi:10.1023/B:MCBI.0000049134.69131.89
14. Diab El-Harakeh M, Njeim R, Youssef A, Youssef N, Eid AA, Bouhadir KH. Novel triazine-based pyrimidines suppress glomerular mesangial cells proliferation and matrix protein accumulation through a ROS-dependent mechanism in the diabetic milieu. *Bioorg Med Chem Lett* 2019;29:1580–1585. doi:10.1016/j.bmcl.2019.04.052
15. Matoba K, Takeda Y, Nagai Y, Yokota T, Utsunomiya K, Nishimura R. Targeting redox imbalance as an approach for diabetic kidney disease. *Biomedicines*. 2020;8:40. doi:10.3390/biomedicines8020040
16. Hayes JD, Dinkova-Kostova AT. The Nrf2 regulatory network provides an interface between redox and intermediary metabolism. *Trends Biochem Sci*. 2014;39:199–218. doi:10.1016/j.tibs.2014.02.002
17. Tian H, Zheng X, Wang H. Isorhapontigenin ameliorates high glucose-induced podocyte and vascular endothelial cell injuries via mitigating oxidative stress and autophagy through the AMPK/Nrf2 pathway. *Int Urol Nephrol*. 2023;55:423–436. doi:10.1007/s11255-022-03325-y
18. Uruno A, Yamamoto M. The KEAP1-NRF2 system and neurodegenerative diseases. *Antioxid Redox Signal*. 2023;38:974–988. doi:10.1089/ars.2023.0234
19. Yao H, Zhang W, Yang F, Ai F, Du D, Li Y. Discovery of caffeoylisocitric acid as a Keap1-dependent Nrf2 activator and its effects in mesangial cells under high glucose. *J Enzy Inhibit Med Chem*. 2021;37:178–188. doi:10.1080/14756366.2021.1998025
20. Vidigal JA, Ventura A. The biological functions of miRNAs: lessons from in vivo studies. *Trends Cell Biol*. 2015;25:137–147. doi:10.1016/j.tcb.2014.11.004
21. Karali M, Banfi S. Non-coding RNAs in retinal development and function. *Hum Genet*. 2019;138:957–971. doi:10.1007/s00439-018-1931-y
22. Rupaimoole R, Slack FJ. MicroRNA therapeutics: towards a new era for the management of cancer and other diseases. *Nat Rev Drug Discov*. 2017;16:203–222. doi:10.1038/nrd.2016.246
23. Liu Y, Usa K, Wang F, et al. MicroRNA-214-3p in the kidney contributes to the development of hypertension. *J Am Soc Nephrol*. 2018;29:2518–2528. doi:10.1681/ASN.2018020117
24. Cheng Y, Wang D, Wang F, et al. Endogenous miR-204 protects the kidney against chronic injury in hypertension and diabetes. *J Am Soc Nephrol*. 2020;31:1539–1554. doi:10.1681/ASN.2019101100
25. Zhou L, Ma J. MIR99AHG/miR-204-5p/TXNIP/Nrf2/ARE signaling pathway decreases glioblastoma temozolomide sensitivity. *Neurotox Res*. 2022;40:1152–1162. doi:10.1007/s12640-022-00536-0
26. Peng F, Li H, Li S, et al. Micheliolide ameliorates renal fibrosis by suppressing the Mtdh/BMP/MAPK pathway. *Lab Invest*. 2019;99:1092–1106. doi:10.1038/s41374-019-0245-6
27. Ma Z, Li L, Livingston MJ, et al. p53/microRNA-214/ULK1 axis impairs renal tubular autophagy in diabetic kidney disease. *J Clin Investig*. 2020;130(9):5011–5026. doi:10.1172/JCI135536
28. Zhong Y, Wang L, Jin R, et al. Diosgenin Inhibits ROS Generation by Modulating NOX4 and mitochondrial respiratory Chain and suppresses apoptosis in diabetic nephropathy. *Nutrients*. 2023;2023:15.
29. Baird L, Yamamoto M. The molecular mechanisms regulating the KEAP1-NRF2 pathway. *Mol Cell Biol*. 2023;2023:40.
30. Ren P, Qian F, Fu L, et al. Adipose-derived stem cell exosomes regulate Nrf2/Keap1 in diabetic nephropathy by targeting FAM129B. *Diabetol Metab Syndr*. 2023;15:149. doi:10.1186/s13098-023-01119-5
31. Xu P, Zhan H, Zhang R, et al. Early growth response factor 1 upregulates pro-fibrotic genes through activation of TGF-β1/Smad pathway via transcriptional regulation of PAR1 in high-glucose treated HK-2 cells. *Mol Cell Endocrinol*. 2023;572:111953. doi:10.1016/j.mce.2023.111953
32. Wang T, Cui S, Liu X, et al. LncTUG1 ameliorates renal tubular fibrosis in experimental diabetic nephropathy through the miR-145-5p/dual-specificity phosphatase 6 axis. *Ren Fail*. 2023;45:2173950. doi:10.1080/0886022X.2023.2173950
33. Xue X, Liu M, Wang Y, et al. MicroRNA-494-3p exacerbates renal epithelial cell dysfunction by targeting SOCS6 under high glucose treatment. *Kidney Blood Pressure Res*. 2022;47:247–255. doi:10.1159/000521647
34. He J, Kang L, Wu T, et al. An elaborate regulation of Mammalian target of rapamycin activity is required for somatic cell reprogramming induced by defined transcription factors. *Stem Cells Dev*. 2012;21:2630–2641. doi:10.1089/scd.2012.0015
35. Yang D, Livingston MJ, Liu Z, et al. Autophagy in diabetic kidney disease: regulation, pathological role and therapeutic potential. *Cell Mol Life Sci*. 2018;75:669–688. doi:10.1007/s00018-017-2639-1
36. Jia Z, Wang K, Zhang Y, et al. Icariin ameliorates diabetic renal tubulointerstitial fibrosis by restoring autophagy via regulation of the miR-192-5p/GLP-1R pathway. *Front Pharmacol*. 2021;12:720387. doi:10.3389/fphar.2021.720387
37. Sui H, Fan S, Liu W, et al. LINC00028 regulates the development of TGFβ1-treated human tenon capsule fibroblasts by targeting miR-204-5p. *Biochem Biophys Res Commun*. 2020;525:197–203. doi:10.1016/j.bbrc.2020.01.096
38. Wu Q, Guan YB, Zhang KJ, Li L, Zhou Y. Tanshinone IIA mediates protection from diabetes kidney disease by inhibiting oxidative stress induced pyroptosis. *J Ethnopharmacol*. 2023;316:116667. doi:10.1016/j.jep.2023.116667
39. Feng T, Li W, Li T, Jiao W, Chen S. Circular RNA_0037128 aggravates high glucose-induced damage in HK-2 cells via regulation of microRNA-497-5p/nuclear factor of activated T cells 5 axis. *Bioengineered*. 2021;12:10959–10970. doi:10.1080/21655979.2021.2001912
40. Jha JC, Gray SP, Barit D, et al. Genetic targeting or pharmacologic inhibition of NADPH Oxidase Nox4 provides renoprotection in long-term diabetic nephropathy. *J Am Soc Nephrol*. 2014;25:1237–1254. doi:10.1681/ASN.2013070810
41. Lan T, Li Y, Fan C, et al. MicroRNA-204-5p reduction in rat hippocampus contributes to stress-induced pathology via targeting RGS12 signaling pathway. *J Neuroinflammation*. 2021;18:243. doi:10.1186/s12974-021-02299-5

42. Su S, Ma Z, Wu H, Xu Z, Yi H. Oxidative stress as a culprit in diabetic kidney disease. *Life Sci*. 2023;322:121661. doi:10.1016/j.lfs.2023.121661
43. Cui W, Li B, Bai Y, et al. Potential role for Nrf2 activation in the therapeutic effect of MG132 on diabetic nephropathy in OVE26 diabetic mice. *Am J Physiol Endocrinol Metab*. 2013;304:E87–E99.
44. Dong J, Zhang KJ, Li GC, et al. CDDO-Im ameliorates osteoarthritis and inhibits chondrocyte apoptosis in mice via enhancing Nrf2-dependent autophagy. *Acta Pharmacol Sin*. 2022;43:1793–1802. doi:10.1038/s41401-021-00782-6
45. Shen Q, Fang J, Guo H, et al. Astragaloside IV attenuates podocyte apoptosis through ameliorating mitochondrial dysfunction by up-regulated Nrf2-ARE/TFAM signaling in diabetic kidney disease. *Free Radic Biol Med*. 2023;203:45–57. doi:10.1016/j.freeradbiomed.2023.03.022
46. Song J, Wang H, Sheng J, et al. Vitexin attenuates chronic kidney disease by inhibiting renal tubular epithelial cell ferroptosis via NRF2 activation. *Mol Med*. 2023;29:147. doi:10.1186/s10020-023-00735-1
47. Zhang J, Xu HX, Zhu JQ, Dou YX, Xian YF, Lin ZX. Natural Nrf2 inhibitors: a review of their potential for cancer treatment. *Int J Biol Sci*. 2023;19:3029–3041. doi:10.7150/ijbs.82401
48. Civantos E, Bosch E, Ramirez E, et al. Sitagliptin ameliorates oxidative stress in experimental diabetic nephropathy by diminishing the miR-200a/Keap-1/Nrf2 antioxidant pathway. *Diabetes Metab Syndr Obes*. 2017;10:207–222. doi:10.2147/DMSO.S132537